

# Utilizing a strait-range green phosphor $\gamma$ -AlON:Mn,Mg for the task of achieving a super-broad hue gamut display

My Hanh Nguyen Thi<sup>1</sup>, Phan Xuan Le<sup>2</sup>

<sup>1</sup>Faculty of Mechanical Engineering, Industrial University of Ho Chi Minh City, Ho Chi Minh City, Vietnam

<sup>2</sup>Faculty of Mechanical-Electrical and Computer Engineering, School of Engineering and Technology, Van Lang University, Ho Chi Minh City, Vietnam

## Article Info

### Article history:

Received Nov 28, 2021

Revised Jun 5, 2022

Accepted Jun 24, 2022

### Keywords:

Color homogeneity

Luminous flux

Monte Carlo theory

WLEDs

$\gamma$ -AlON:Mn,Mg

## ABSTRACT

The screen backlighting produced by green  $\beta$ -sialon:Eu, as well as red  $K_2SiF_6:Mn$  phosphors, have an extremely expansive hue gamut that encompasses the majority of the national television system committee (NTSC) triangle. For our research, a substitute phosphor in green would be probed in terms of improving the screen hue range even further. The phosphor  $\gamma$ -AlON:Mn,Mg appears to be green in color with a smaller radiation band of colors than sharp  $\beta$ -sialon:Eu. By replacing  $\gamma$ -AlON:Mn,Mg with  $\beta$ -sialon:Eu, the screen hue range in the blue-green area is significantly expanded. In both the International Commission on Illumination (CIE) 1931 and CIE 1976 hue spaces, the hue range of screens with  $\gamma$ -AlON:Mn,Mg, and  $K_2SiF_6:Mn$  entirely surpasses the NTSC benchmark. Furthermore, the stability of LEDs emit white light using  $\gamma$ -AlON:Mn,Mg appears to be similar to LEDs that utilize  $\beta$ -sialon:Eu.

This is an open access article under the [CC BY-SA](https://creativecommons.org/licenses/by-sa/4.0/) license.



## Corresponding Author:

Phan Xuan Le

Faculty of Mechanical-Electrical and Computer Engineering, School of Engineering and Technology

Van Lang University

Ho Chi Minh City, Vietnam

Email: le.px@vlu.edu.vn

## 1. INTRODUCTION

Over the last few decades, the technical propensities of liquid crystal displays (LCDs) are still highly concentrated on improving resolution as well as energy usage. Even so, the expansion of the hue range has received less interest. Most television yields have a hue range that covers 70% of the NTSC benchmark [1], [2]. On the contrary, in the latest days, there has been a quick rise in the need for a broader hue range, and TV yields having a broader hue range encompassing the entire NTSC triangle are now on the marketing. Furthermore, as clarified in Recommendation ITU-R BT.2020, TV with an excellent definition has a broader hue space coverage than traditional broad-hue-gamut benchmarks such as NTSC [3], [4]. In this context, the hue ranges of backlighting gadgets have to be vastly gotten better to satisfy the novel requirement. Because of the sharp and dissymmetrical radiation spectral shape, and also the high stability,  $\beta$ -sialon ( $Si_{6-z}Al_zO_zN_{8-z}$ ):Eu is considered a good potential phosphor in green for the broad-hue-gamut white light-emitting diode (WLED) backlighting formation [5], [6]. Utilizing  $\beta$ -sialon:Eu having inferior z results (following will be called sharp  $\beta$ -sialon:Eu) can further broaden the screen hue range [7], [8]. Screens that utilize  $\beta$ -sialon:Eu ( $z = 0.05$ ) as well as  $K_2SiF_6:Mn$ , have an extremely broad hue gamut that encompasses the majority of the NTSC triangle. Nevertheless, this hue gamut is much lower to the new benchmark and must be significantly improved. It is crucial to look for a green phosphor alternative that offers a significantly shorter as well as thinner radiation band of colors for this purpose [9], [10]. On blue lighting stimulation,  $Mn^{2+}$ -doped  $\gamma$ -AlON

has a radiation peak measured at 520 nm along with a fullwidth at half maximum measured at 44 nm, resulting in a shorter, thinner radiation spectrum, compared to  $\beta$ -sialon:Eu. Furthermore,  $Mg^{2+}$  codoping greatly enhances the brightness of  $Mn^{2+}$ -doped  $\gamma$ -AlON. Moreover, the quantum efficacy for the co-doped specimen exceeds 60% below 445 nm stimulation. The good potential luminescence characteristics imply  $\gamma$ -AlON:Mn,Mg can be a potential phosphor in green used to accomplish broader hue ranges. The luminescence characteristics of  $\gamma$ -AlON:Mn,Mg would be maximized in this research by manipulating its chemical components. The optic characteristics and reliability of white light emitting diode (LED) backlighting gadgets made with strait-range green  $\gamma$ -AlON:Mn,Mg, and red  $K_2SiF_6$ :Mn phosphors are probed.

## 2. EXPERIMENTAL METHODS

The simulation of the spectrum was first performed to get a concept of the satisfactory radiation band of colors of a green-color phosphor for the broad-hue-gamut screens in the future. In summary, a blue LED chip's spectra with a maximum point under 445 nm, a phosphor in green, as well as a phosphor in red, yielded a white LED spectrum. The evaluated band of colors of  $K_2SiF_6$ :Mn was utilized as the red phosphor's spectrum, as well as the evaluated spectrum in  $\beta$ -sialon:Eu or a premeditated Gaussian band of colors having different maximum wavelengths ( $\lambda_p$ ) or half widths would be utilized in the form of the green phosphor's color band. The theoretical limitation of illuminating effectiveness was calculated on the premise phosphors' interior quantum effectiveness appeared to be 100%, i.e., with Stokes' loss solely considered. The attributes of a screen were explored by overlapping the radiation band of colors in WLED as well as the transmission in an LCD screen with red-green-blue sievers as well as liquid crystals. The transference spectra for a siever are depicted in Figure 1. The screen luminosity is described as the visibility of the screen's white illumination. With the international commission on illumination (CIE) benchmark for WLED, the chromaticity coordinates ( $x$ ;  $y$ ) are defined in a way for the correlated color temperature (CCT) in the screen white point to reach 10,000 K [11], [12].

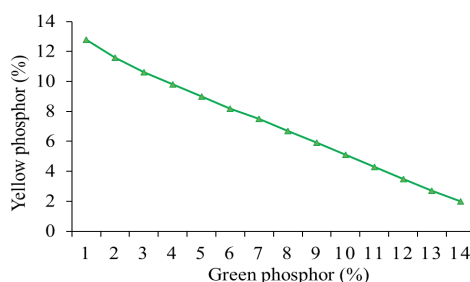


Figure 1. Altering phosphor concentration for the task of maintaining the mean CCT

## 3. RESULTS AND DISCUSSION

When creating a white LED, it is important to first determine the sort of light source that will be used. In general, high color rendering necessitates emission throughout a considerable portion from the observable spectrum, which yields an efficiency penalty, and vice versa: appropriate (quasi)monochromatic sources can achieve very high efficiency. Obtaining great hue output or desirable performance are disparate tasks, and the paper would demonstrate this later. There are color quality scale (CQS) and radiated luminous efficacy (LER) aimed at three possible illuminations with emission bands in Gaussian form as well as a full width at half maximum (FWHM) measured at 10 nm. The initial (blue) light source's peak emission wavelength was set under 460 nm to balance the adequate short-wavelength emission as well as maintain acceptable sight responsiveness. We made this decision as shorter wavelengths reduce sight responsiveness greatly. Furthermore, 460 nm would be the top wavelength most commonly seen in blue LED devices, as well as the wavelength in common WLED devices that utilize YAG:Ce transmutation. The top emission wavelengths in the other illuminations were altered between 510 and 570 nm as well as 580 and 700 nm, respectively. We modified the illumination strength for each combination to produce a white illumination that yields a warm CCT measured at 3000 K that can be a substitute for traditional lights along with no divergence from the black body locus [13]-[15]. For each distribution, we calculated the CQS as well as LER. The same procedure was followed in the case of white illumination that yields a CCT measured at 4500 K. When it comes to 3000 K, selecting the green illumination between 530 and 545 nm as well as the red illumination between 605 and 615 nm results in a relatively limited zone in which the CQS reaches 70. Such a result would not become typical uses for the optical field. It is possible to achieve an LER result measured at 400 lm/W inside the stated range. Said result would be roughly the maximum result attainable in a white

illumination. With 4500 K, the outcomes would be essentially the same, yielding an identical CQS as well as a faintly smaller LER value, a result of the significantly greater involvement from the blue discharge band, rousing less sight response. These narrow emission bands, as will be detailed further, nicely imitate the discharge from various rare earth metals with three valences 4f–4f discharge bands (for example,  $Tb^{3+}$  under 540 nm or  $Eu^{3+}$  under 615 nm) [16]-[18].

Because a decent hue output appears to be impossible to obtain under a tiny amount of thin discharge apexes, the usage for 4f–4f line emitters appears to be not appropriate enough when it comes to generating significant hue output. On the other hand, LER results may reach high levels, making those an excellent option when it comes to displays like LCDs that utilize LEDs in the form of backlights. Hue saturation for basic hues sorely matters in this scenario. Obviously, no reasonable color rendering can be accomplished with three narrow light sources. The CQS ought to be ideally in the upper 80s or low 90s. As a result, we simulated three potential illuminations of blue, green, and red having FWHMs measured at 30 nm, 50 nm, and 70 nm as a second scenario, which would be reasonable estimates in the case of phosphors treated with  $Eu^{2+}$ . Because a blue LED's FWHM often reaches near 30 nm, this approach also applies to blue LED pumped white LEDs. If the green discharge line reaches 525 nm along with the red discharge line reaching 610 nm, a CQS value exceeding 90 is readily attainable, accompanied by an LER value reaching 300 lm/W. Furthermore, there is a rather big zone in which the CQS would be greater than 85, allowing for modifications in the correct apex location as well as the form in the discharge lines of the phosphors. A CQS of (almost) 100 can be attained by using even larger bands. However, an efficiency penalty will occur, caused by an increased number of photons generated by the observable spectrum's polar sides that rouse less sight response. Nonetheless, a discharge spectrum that yields huge CQS results greater than 95, as well as an LER reaching 250 lm/W, is achievable. Carrying out an identical examination using an FWHM measured at 30 nm in the case of the three illuminations results in a maximal CQS and stands for color rendering index (CRI) in the mid-80s as well as an LER reaching 350 lm/W maximumly [19]-[21]. As a result, smart illuminations from the three LED devices may produce white illumination that yields adequate hue representation for a variety of practical uses. However, when the requirement includes strong hue generation, a fourth LED device must be added.

It should be noted that recent research made an identical computation concerning the relationship among discharge wavelengths as well as hue generation. However, only narrowband (line) emitters were examined in this scenario. The standard CRI color rendering index, considered inaccurate for describing narrowband sources, was also utilized. Hue regeneration accompanied by narrowband sources is clearly dependent on the precise discharge wavelengths in the case of specimens with a quickly shifting reflectance spectrum. With this taken into account, specimens such as tomatoes prove to be exceptionally challenging to accurately envision. Assume that we have appropriate phosphors, it is possible to generate illuminations yielding varying hue temperatures via adjusting the mass proportion among the disparate phosphors (as well as in the case of a blue pumping LED, also the overall loading) [22]. This may be shown by noting the comparatively large cross-section in the zones that have significant hue generation, in the case of CCT values measured at 3000 K as well as 4500 K.

When it comes to general illumination, we can only use most LED or WLED devices. These devices are commercially available, for example, in the form of backlights in LCDs, which substitutes for fluorescent bulbs. The said LED devices would emit a considerable amount of light within the blue, green, as well as red parts from the emission spectrum, and then brilliant and saturated colors would be kept after filtering. Hue temperature, hue generation, as well as divergence from the black body locus would be of lesser importance in this instance. For backlight purposes, Zhou *et al.* [23] came up with a technique of transmutation involving two phosphors (by utilizing a blue LED green  $\beta$ -sialon: $Eu^{2+}$  with FWHM measured at 55 nm as well as red  $CaAlSiN_3:Eu^{2+}$ ) for the task of achieving a hue scale reaching 92% of the NTSC standard.

In Figure 1, we can see the markedly opposite change between the concentrations of green phosphorus  $\gamma$ -AlON:Mn, Mg and yellow phosphorus YAG: $Ce^{3+}$ . We have two important implications when there is this change, one is to affect the absorptivity and dispersing in the WLED of the two phosphor films, the other is to maintain the average level of the CCT. In addition, it determines the hue standard and luminous flux efficiency of the WLED. From the above-mentioned implications, the selection of  $\gamma$ -AlON:Mn, Mg concentration is the foundation for determining the color quality of WLEDs. When  $\gamma$ -AlON:Mn, Mg increases (2-20% Wt.) then the YAG: $Ce^{3+}$  concentration must be reduced for the task of sustaining the average CCT. We have the same analogy when it comes to WLEDs that have different hue temperatures from 5600-8500 K.

Figure 2 illustrates the calculated optic characteristics of the screens based on the simulated band of colors in the green-color phosphor. The bar shown by Figure 2 represents an expanded bar for the displayed plot having  $\beta$ -sialon:Eu. To make broad-hue-gamut screens practicable and generally applicable in the future, it is critical to select an acceptable green radiation spectrum that does not significantly reduce the screen

brightness when compared to screens having  $\beta$ -sialon:Eu. The green radiation spectra shown above the top part for the bar shown by Figure 2 will be selected for this reason. A maximum wavelength exceeding 520 nm as well as a half-maximum breadth below 45 nm would be greatly desirable to use broad-hue-gamut screens in the future. The transmission spectrum of WLEDs is shown in Figure 2 along with the concentration of green phosphor  $\gamma$ -AlON:Mn,Mg. We can decide depending on the requirements of the manufacturers. WLEDs that demand good hue fidelity can diminish lighting flux by a tiny amount. When white light is employed, the spectral area synthesis displayed in Figure 2 can be seen. The spectrum of 5000 K is depicted in the five figures below. It is obvious that the two sections of the light spectrum, 420-480 nm as well as 500-640 nm, tend to have their intensities increase with  $\gamma$ -AlON:Mn, Mg concentration, particularly the spectra at  $\sim$ 550 nm.

The expansion in the two-range radiation spectrum represents an improvement in the output illuminating beam. Furthermore, if the scattering of blue illumination in the WLED grows, the dispersion within the phosphor sheet as well as within the WLED device will be increased. This leads to color uniformity becoming more popular. At high temperatures, it will be hard to control the hue homogeneity of the distant phosphor configuration [24], [25]. This is a significant outcome when utilizing  $\gamma$ -AlON:Mn,Mg. Therefore, this study indicates that  $\gamma$ -AlON:Mn,Mg may be able to improve the hue quality of WLEDs at small as well as huge hue heats (5600 K and 8500 K). Therefore, the generated light flux efficiency of this bilayer distal phosphor layer has been demonstrated in the paper. The data in Figure 3 show that when the  $\gamma$ -AlON:Mn,Mg concentration was raised from 2% wt. up to 20% wt. there will be a significant increase in the luminous flux.

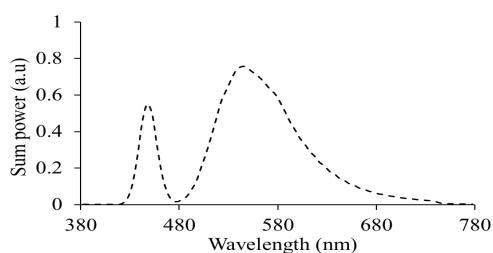


Figure 2. The radiation band of colors of 5000 K WLED device along with  $\gamma$ -AlON:Mn,Mg concentration

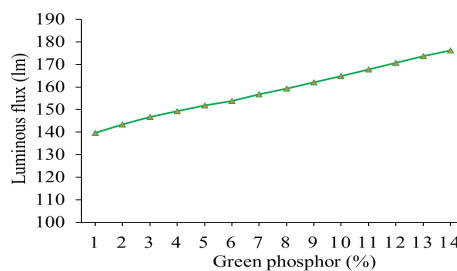


Figure 3. The luminous flux of the WLED device along with  $\gamma$ -AlON:Mn,Mg concentration

In Figure 4, when using phosphor concentrations  $\gamma$ -AlON:Mn,Mg, the hue deviation was significantly reduced in all three mean CCTs. The absorptivity of the red phosphor film is the reason for this. When the blue illumination generated by the LED chip gets absorbed via  $\gamma$ -AlON:Mn,Mg phosphor, the blue lighting is converted to green illumination. Besides the blue light generated by the chip, the yellow light will be absorbed by the  $\gamma$ -AlON:Mn,Mg particles. Even so, the absorptivity of blue lighting from the LED chip is larger than these two absorptions due to the absorption features of the different materials. When we add  $\gamma$ -AlON:Mn,Mg, the green light content in WLEDs will increase. This improves the hue uniformity index. The higher the hue uniformity index, the more expensive the WLED white light. Therefore, hue uniformity is currently one of the most important criteria among WLED parameters. In contrast, the  $\gamma$ -AlON:Mn,Mg cost would be very cheap. This is why  $\gamma$ -AlON:Mn,Mg is being used for many different applications lately.

The hue quality excellence cannot be determined with a high hue uniformity index alone as hue uniformity is simply a factor to consider when evaluating the hue quality of WLEDs. Instead, the researchers went on to develop a hue rendering index and hue quality scale. When the hue rendering index is illuminated by light, it evaluates the true hue of a thing. When the amount of green light is too much between the three main hues: blue, yellow, and green, it will cause an imbalance of hue. This reduces hue fidelity, leading to a rather serious impact on the hue quality of WLED. Whenever the phosphorus layer is distant from  $\gamma$ -AlON:Mn,Mg, a small penalty for CRI occurs, as can be seen via Figure 5. On the other hand, CRIs are allowed as they are just a gap in the CQS. Among CRI and CQS, the CQS is an indicator that is more necessary and harder to achieve. CQS is an index carrying three quite important facets: hue rendering index, viewer's choice, as well as hue coordinate. CQS is considered an overall indicator of hue quality. Figure 6 shows the increase of CQS in the presence of a distant  $\gamma$ -AlON:Mn,Mg phosphor layer. More remarkable, when increasing the concentration of  $\gamma$ -AlON:Mn,Mg, CQS did not change much when the concentration of  $\gamma$ -AlON:Mn,Mg was under 10% wt. And when the concentration of  $\gamma$ -AlON:Mn,Mg exceeds 10% wt. then

CRI, along with CQS, is significantly reduced owing to severe hue loss in case the green hue of  $\gamma$ -AlON:Mn,Mg takes up too much. In general, when using green phosphor  $\gamma$ -AlON:Mn,Mg, careful consideration must be given to choosing an appropriate concentration.

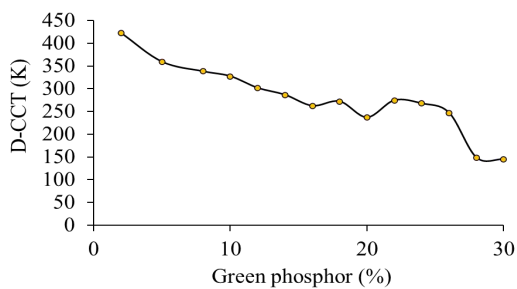


Figure 4. The hue deviation of the WLED device along with  $\gamma$ -AlON:Mn,Mg concentration

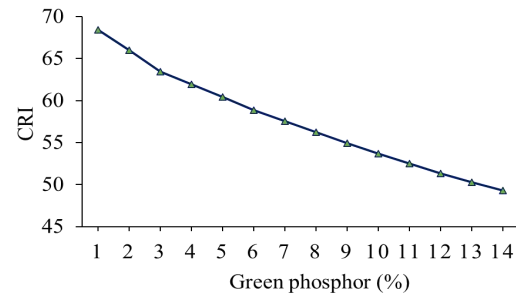


Figure 5. The hue rendering indicator of the WLED device along with  $\gamma$ -AlON:Mn,Mg concentration

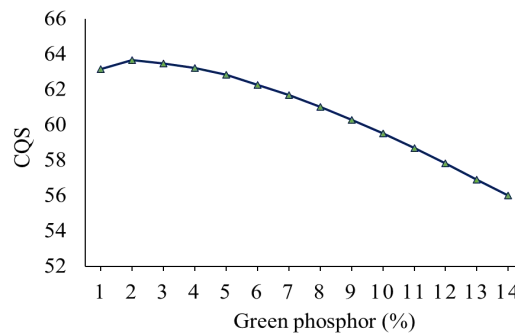


Figure 6. The hue standard scale of the WLED device along with  $\gamma$ -AlON:Mn,Mg concentration

#### 4. CONCLUSION

In brief, utilizing  $\gamma$ -AlON:Mn,Mg having a shorter as well as thinner radiation band of colors, it was possible to successfully enhance a broad hue range and dependable white LEDs. White LED backlighting systems based on  $\gamma$ -AlON:Mn,Mg provide a hue range of more than 100% of the NTSC benchmark, as well as good dependability similar to that achieved with sharp  $\beta$ -sialon:Eu as well.

#### ACKNOWLEDGEMENTS

This study was financially supported by Van Lang University, Vietnam.





#### REFERENCES

- [1] D. Yan, S. Zhao, H. Wang, and Z. Zang, "Ultrapure and highly efficient green light emitting devices based on ligand-modified CsPbBr<sub>3</sub> quantum dots," *Photonics Research*, vol. 8, no. 7, pp. 1086-1092, 2020, doi: 10.1364/PRJ.391703.
- [2] J. Cheng *et al.*, "Luminescence and energy transfer properties of color-tunable Sr<sub>4</sub>La(PO<sub>4</sub>)<sub>3</sub>O: Ce<sup>3+</sup>, Tb<sup>3+</sup>, Mn<sup>2+</sup> phosphors for WLEDs," *Optical Materials Express*, vol. 8, no. 7, pp. 1850-1862, 2018, doi: 10.1364/OME.8.001850.
- [3] C. Zhang, L. Xiao, P. Zhong, and G. He, "Photometric optimization and comparison of hybrid white LEDs for mesopic road lighting," *Applied Optics*, vol. 57, no. 16, pp. 4665-4671, 2018, doi: 10.1364/AO.57.004665.
- [4] Z. Zhao, H. Zhang, S. Liu, and X. Wang, "Effective freeform TIR lens designed for LEDs with high angular color uniformity," *Applied Optics*, vol. 57, no. 15, pp. 4216-4221, 2018, doi: 10.1364/AO.57.004216.
- [5] Z. Wen *et al.*, "Fabrication and optical properties of Pr<sup>3+</sup>-doped Ba (Sn, Zr, Mg, Ta) O<sub>3</sub> transparent ceramic phosphor," *Optics Letters*, vol. 43, no. 11, pp. 2438-2441, 2018, doi: 10.1364/OL.43.002438.
- [6] C. J. C. Smyth, S. Mirkhanov, A. H. Quarterman, and K. G. Wilcox, "27.5 W/m<sup>2</sup> collection efficiency solar laser using a diffuse scattering cooling liquid," *Applied Optics*, vol. 57, no. 15, pp. 4008-4012, 2018, doi: 10.1364/AO.57.004008.
- [7] Z. Song, T. Guo, X. Fu, and X. Hu, "Residual vibration control based on a global search method in a high-speed white light scanning interferometer," *Applied Optics*, vol. 57, no. 13, pp. 3415-3422, 2018, doi: 10.1364/AO.57.003415.
- [8] C. McDonnell, E. Coyne, and G. M. O'Connor, "Grey-scale silicon diffractive optics for selective laser ablation of thin conductive films," *Applied Optics*, vol. 57, no. 24, pp. 6966-6970, 2018, doi: 10.1364/AO.57.006966.





- [9] S.-R. Chung, C.-B. Siao, and K.-W. Wang, "Full color display fabricated by CdSe bi-color quantum dots-based white light-emitting diodes," *Optical Materials Express*, vol. 8, no. 9, pp. 2677-2686, 2018, doi: 10.1364/OME.8.002677.
- [10] J. Zhang, L. Zhao, X. Bian, and G. Chen, "Ce<sup>3+</sup>/Mn<sup>2+</sup>-activated Ca<sub>7</sub>(PO<sub>4</sub>)<sub>2</sub>(SiO<sub>4</sub>)<sub>2</sub>: efficient luminescent materials for multifunctional applications," *Optics Express*, vol. 26, no. 18, pp. A904-A914, 2018, doi: 10.1364/OE.26.00A904.
- [11] T. Kozacki, M. Chlipala, and H.-G. Choo, "Fourier rainbow holography," *Optics Express*, vol. 26, no. 19, pp. 25086-25097, 2018, doi: 10.1364/OE.26.025086.
- [12] C. Han *et al.*, "Effect of surface recombination in high performance white-light CH<sub>3</sub>NH<sub>3</sub>PbI<sub>3</sub> single crystal photodetectors," *Optics Express*, vol. 26, no. 20, pp. 26307-26316, 2018, doi: 10.1364/OE.26.026307.
- [13] Z. Huang *et al.*, "Towards an optimum colour preference metric for white light sources: a comprehensive investigation based on empirical data," *Optics Express*, vol. 29, no. 5, pp. 6302-6319, 2021, doi: 10.1364/OE.413389.
- [14] M. R. Edwards *et al.*, "A multi-terawatt two-color beam for high-power field-controlled nonlinear optics," *Optics Letters*, vol. 45, no. 23, pp. 6542-6545, 2020, doi: 10.1364/OL.403806.
- [15] P. Kaur, Kriti, Rahul, S. Kaur, A. Kandasami, and D. P. Singh, "Synchrotron-based VUV excitation-induced ultrahigh quality cool white light luminescence from Sm-doped ZnO," *Optics Letters*, vol. 45, no. 12, pp. 3349-3352, 2020, doi: 10.1364/OL.395393.
- [16] C. Bai *et al.*, "Full-color optically-sectioned imaging by wide-field microscopy via deep-learning," *Biomedical Optics Express*, vol. 11, no. 5, pp. 2619-2632, 2020, doi: 10.1364/BOE.389852.
- [17] R. E. O'Shea, S. R. Laney, and Z. Lee, "Evaluation of glint correction approaches for fine-scale ocean color measurements by lightweight hyperspectral imaging spectrometers," *Applied Optics*, vol. 59, no. 7, pp. B18-B34, 2020, doi: 10.1364/AO.377059.
- [18] B. Li *et al.*, "High-efficiency cubic-phased blue-emitting Ba<sub>3</sub>Lu<sub>2</sub>B<sub>6</sub>O<sub>15</sub>:Ce<sup>3+</sup> phosphors for ultraviolet-excited white-light-emitting diodes," *Optics Letters*, vol. 43, no. 20, pp. 5138-5141, 2018, doi: 10.1364/OL.43.005138.
- [19] X. Huang, S. Wang, B. Li, Q. Sun, and H. Guo., "High-brightness and high-color purity red-emitting Ca<sub>3</sub>Lu(AlO)<sub>3</sub>(BO<sub>3</sub>)<sub>4</sub>:Eu<sup>3+</sup> phosphors with internal quantum efficiency close to unity for near-ultraviolet-based white-light-emitting diodes," *Optics Letters*, vol. 43, no. 6, pp. 1307-1310, 2018, doi: 10.1364/OL.43.001307.
- [20] J. Zhao *et al.*, "High stability ultra-narrow band self-activated KGaSiO<sub>4</sub> long-persistent phosphors for optical anti-counterfeiting," *Optics Letters*, vol. 46, no. 16, pp. 3829-3832, 2021, doi: 10.1364/OL.429877.
- [21] Q. Zhang, R. Zheng, J. Ding, and W. Wei, "Excellent luminous efficiency and high thermal stability of glass-in-LuAG ceramic for laser-diode-pumped green-emitting phosphor," *Optics Letters*, vol. 43, no. 15, pp. 3566-3569, 2018, doi: 10.1364/OL.43.003566.
- [22] X. Liu *et al.*, "Upconversion luminescence, intrinsic optical bistability, and optical thermometry in Ho<sup>3+</sup>/Yb<sup>3+</sup>: BaMoO<sub>4</sub> phosphors," *Chinese Optics Letters*, vol. 17, no. 11, p. 111601, 2019, doi: 10.3788/COL201917.111601.
- [23] Z. Zhou, G. Liu, J. Ni, W. Liu, and Q. Liu, "White light obtainment via tricolor luminescent centers and energy transfer in Ca<sub>3</sub>ZrSi<sub>2</sub>O<sub>9</sub>:Eu<sup>3+</sup>,Bi<sup>3+</sup>,Tb<sup>3+</sup> phosphors," *Optical Materials Express*, vol. 8, no. 11, pp. 3526-3542, 2018, doi: 10.1364/OME.8.003526.
- [24] J. Cheng *et al.*, "Photoluminescence properties of Ca<sub>4</sub>La<sub>6</sub>(SiO<sub>4</sub>)<sub>4</sub>(PO<sub>4</sub>)<sub>2</sub>O<sub>2</sub>-based phosphors for wLEDs," *Chinese Optics Letters*, vol. 17, no. 5, p. 051602, 2019.
- [25] L. Xiao, C. Zhang, P. Zhong, and G. He, "Spectral optimization of phosphor-coated white LED for road lighting based on the mesopic limited luminous efficacy and IES color fidelity index," *Applied Optics*, vol. 57, no. 4, pp. 931-936, 2018, doi: 10.1364/AO.57.000931.

## BIOGRAPHIES OF AUTHORS



**My Hanh Nguyen Thi**     received a Bachelor of Physics from an Giang University, VietNam, Master of Theoretical Physics And Mathematical Physics, Hanoi National University of Education, VietNam. Currently, she is a lecturer at the Faculty of Mechanical Engineering, Industrial University of Ho Chi Minh City, Viet Nam. Her research interests are Theoretical Physics and Mathematical Physics. She can be contacted at email: nguyenthimyanh@iuh.edu.vn.



**Phan Xuan Le**     received a Ph.D. in Mechanical and Electrical Engineering from Kunming University of Science and Technology, Kunming city, Yunnan province, China. Currently, He is a lecturer at the Faculty of Engineering, Van Lang University, Ho Chi Minh City, Viet Nam. His research interests are Optoelectronics (LED), Power transmission and Automation equipment. He can be contacted at email: le.px@vlu.edu.vn.